Gagné *et al. Water Emerg Contam Nanoplastics* 2024;3:4
DOI: 10.20517/wecn.2023.60

Water Emerging Contaminants & Nanoplastics

Research Article

Open Access

Simple detection of polystyrene nanoparticles and effects in freshwater mussels: method development and *in situ* application to urban pollution

François Gagné, Maxime Gauthier, Chantale André

Aquatic Contaminants Research Division, Environment and Climate Change Canada, Montréal H2Y 1E7, Québec, Canada.

Correspondence to: Prof. François Gagné, Aquatic Contaminants Research Division, Environment and Climate Change Canada, 105 McGill, Montréal H2Y 1E7, Québec, Canada. E-mail: francois.gagne@ec.gc.ca

How to cite this article: Gagné F, Gauthier M, André C. Simple detection of polystyrene nanoparticles and effects in freshwater mussels: method development and *in situ* application to urban pollution. *Water Emerg Contam Nanoplastics* 2024;3:4. https://dx.doi.org/10.20517/wecn.2023.60

Received: 4 Oct 2023 **First Decision:** 29 Nov 2023 **Revised:** 6 Dec 2023 **Accepted:** 15 Dec 2023 **Published:** 21 Dec 2023

Academic Editors: Damià Barceló, Mohammad Hadi Dehghani **Copy Editor:** Pei-Yun Wang **Production Editor:** Pei-Yun Wang

Abstract

The ubiquity of plastics in environments worldwide is raising concerns about their toxicity to organisms. The purpose of this study was to investigate simple means to determine the exposure and effects of nanoplastics (NPs) in the freshwater mussels *Elliptio complanata* (*E. complanata*). NP tissue levels were determined using a plasmonic nanogold sensor probe and effects were determined using the refractive index (RI) and thiol-reaction rates (TRR) in protein-dense tissue extracts. This method was adapted to quantitatively measure the concentration of NPs in tissues using a salting-out extraction in the presence of acetonitrile (ACN). Concentrated solutions of albumin were first spiked with NPs to evaluate changes in RI and TRR to determine crowding effects. The data revealed that NPs readily decreased the RI and TRR in albumin *in vitro*. These three simple assays were then applied on freshwater mussels caged for 3 months at various sites in a largely populated area. Mussels downstream of the city center and found at the street runoff discharge sites were highly contaminated by NPs and the RI and TRR were also reduced. In conclusion, simple and readily accessible assays to assess the NP contamination based on a visual nanogold sensor technology, and the effects of plastics are proposed for freshwater mussels.

Keywords: Polystyrene nanoplastics, nanogold sensor probe, refractive index, thiol-reaction rates, *Elliptio complanata*, municipal effluents

INTRODUCTION

Plastic materials are commonly found in many objects in our daily lives, such as clothing, personal care products, food packages, and drink containers. They provide numerous benefits in the fabrication of domestic and industrial products owing to properties such as their relative inertness, lightweightness, resistance to shock, and low cost of production[1]. Given the global and exponential consumption of plastics and the limited regulation of plastic waste disposal, it is estimated that five trillion fragments exceeding weights of 250,000 tons of plastics already found their way into oceans[2]. In the environment, plastics are gradually degraded into smaller particles termed microplastics (MPs, for sizes between 5 mm to 1 μm) and nanoplastics (NPs, for sizes between 1-1,000 nm[3]). The small size and high surface area of NPs make their analysis tedious in various environmental compartments[4,5]. While MPs are commonly analyzed using microscopic Fourier transform infrared, Raman spectroscopy, and thermo-analytical methods, NPs represent an ongoing challenge. At the moment, methods to detect NPs, which behave differently than MPs and dissolved contaminants, are lacking for organisms. Traditionally, methods used to study plastics involve specialized imaging techniques, separation by chromatographic/field flow techniques, and infrared spectroscopy. An important proportion of plastic materials are retained by municipal effluents and ongoing studies examine ways to remove and degrade plastic on-site[6]. These processes involve separation approaches such as absorption, filtration, and advanced oxidation to separate and degrade these materials at the wastewater treatment plant. The wide range of particle sizes adds to the complexity of global plastic contamination and raises questions as to the ability of the ecosystem to tolerate this pollution on such a large scale. In opposition to MPs, NPs can diffuse across cellular membranes and may perturb cellular physiology. A recent review highlighted that NPs are bioavailable and lead to oxidative stress, inflammation, and potentially cancers[7]. Hence the ability of NPs to diffuse across biological membranes and their ubiquity in the environment may pose risks to the sustainability of aquatic ecosystems and need to be further addressed.

The accumulation of NPs in crowded intracellular compartments can disrupt the complex fractal organization of protein networks[8,9], resulting in the loss of protein function and ultimately impair enzyme activity. These interactions involving hydrophobic surfaces of NPs and local ionic properties of proteins can result in the coating of various proteins [e.g., lysozyme, albumin, and lactate dehydrogenase (LDH)] and can lead to changes in the protein organization. During the aging of NPs, the hydrophobic surface is oxidized by UV or ozone-forming carboxylates at the surface, which can also add to the interaction with the hydrophobic and local positive charges of proteins[10]. The refractive index (RI) of proteins represents a simple and cheap analytical measure to determine the changes in protein concentration, conformation, and composition[11,12]. Changes in the RI per protein mass reveal changes in the conformation and composition of proteins at concentration scales approaching those found in cells (100-400 mg/mL). Within this concentration range, free diffusion of solutes is restricted and could expectedly limit enzyme-catalyzed reaction rates. For example, the LDH activity was decreased by polystyrene (Ps) NPs (PsNPs) of 100 nm diameter[13]. In turn, decreased LDH activity was also reflected by a reduced affinity for pyruvate co-substrate (higher K_M) owing to the reduced fractal dimension of LDH kinetics. Cytoplasmic proteins and lipids could agglomerate during sustained oxidative stress, forming insoluble complexes associated with age-related pigments or lipofuscins[14]. Mediterranean mussels exposed for 7 days to plastic and tire rubber leachates showed elevated levels of oxidative damage and loss of lysosomal stability with increased levels of lipid peroxidation and lipofuscins. When β-amyloid proteins (or other proteins with β-sheet conformation) undergo oxidative degradation, they form insoluble plaques involved with neurodegeneration and amyloidosis in various organs and tissues[15]. Hence, the evaluation of amyloids in organisms exposed to pollution could prove a useful chronic toxicity biomarker associated with the disruption in protein organization in the cytoplasm. These changes could be easily determined by measuring (1) the changes in

RI in concentrated protein suspensions; and (2) the formation of 2-nitro-5-thiobenzoate (TNB), which is produced by the reaction between free thiols and 5,5-dithio-bis-2-nitrobenzoic acid (DTNB). The basis of these simple assays consists of the measurements of the reorganization of dense protein networks by NPs that influence the RI and lower the enzymatic reaction rate in a restricted diffusion microenvironment.

This study aimed to suggest simple and quick markers for the assessment of exposure and effects of PsNPs in aquatic organisms. For this study, we chose a freshwater mussel *Elliptio complanata* (*E. complanata*), endemic to the Saint-Lawrence River, as a sentinel species to reflect the NP contamination in various urban contexts. To assess the exposure of mussels to NPs, a newly developed plasmonic nanogold (nAu) sensor probe allowing the visual detection and quantitation of NPs, requiring only a cell phone camera and free application for color analysis[16], was adapted in biological tissues. Effects of NPs were determined by changes in the RI and thiol-reaction rates (TRR) first with concentrated solutions of albumin *in vitro*. We also tested these markers, along with neutral lipids, aldehydes, and amyloids, in the previously exposed *E. complanata*. These methods were applied to experimentally caged mussels (1) downstream of a large city; (2) in a municipal effluent dispersion plume; (3) at a rainfall/road overflow site, which is an important source of tire wear nanoparticles (TWNPs); and (4) in a pristine lake for comparisons.

MATERIAL AND METHODS

In vitro effects of polystyrene nanoparticles

The influence of PsNPs on the RI and TRR in concentrated albumin was examined *in vitro* to highlight potential biophysical properties of interest in the development of NP biomarkers. A solution of bovine serum albumin (100 mg/mL; MilliporeSigma Canada Ltd., Oakville, Canada), which corresponds to the concentration range of proteins in eucaryotic cell cytoplasm[17] (100-400 mg/mL), was prepared in phosphate-buffered saline (PBS, 140 mM NaCl, 1 mM KH_2PO_4, 1 mM $NaHCO_3$, pH 7.4). The aliquots of 200 µL were exposed to increasing concentrations of PsNPs (0, 0.05, 0.1, and 0.15 µg/mL; Polyscience Inc, Warrington, USA) for 5 min at RT. The PsNPs were uncoated spheres with a diameter of 20 nm, and dilutions were prepared in MilliQ deionized water to limit aggregation. The RI was determined in the albumin-rich solutions using PBS as blank (RI = 1.3326) using an electronic RI device (HDR-P5, Fisher brand, Canada). This preliminary experiment revealed that PsNPs alone did not influence the RI. Then, the TRR was determined by adding 20 µL of 1 mM 5,5'-dithiobis-2-nitrobenzoate (DTNB; MilliporeSigma Canada Ltd., Oakville, Canada) to 200 µL of albumin concentrate[18]. The absorbance was recorded at 412 nm using a microplate reader (model: Synergy-4, Bioteck Instruments, Winooski, USA) for 15 min with 30 s intervals.

Gold nanoparticle - mercaptoundecanoic acid assay

The detection of NPs was achieved using a recently developed nAu plasmonic sensor methodology initially designed for the visualization of NPs in drinking water and from the leaching of heated tea bags or other materials[16]. This methodology was adapted to biological tissues by introducing a preliminary PsNPs salting-out extraction step and recuperation with acetonitrile (ACN) as previously described[19]. The nAu suspension (mean diameter of particles: 14 nm) was commercially obtained from nanoComposix (San Diego, USA) as 50 µg/mL suspension containing 1 mM citrate. The nAu suspension (10 mL) was treated with 0.01% mercaptoundecanoic acid (MUA; prepared in ethanol 100%) for 12 h at RT in the dark to allow binding of the lipophilic acid MUA to nAu to form nAu-MUA complexes [Figure 1]. This solution was filtered through a 0.22 µm cellulose membrane and centrifuged (15,000 × *g*, at 20 °C) for 5 min. The supernatant was discarded, and the pellet was resuspended in half the volume (5 mL) of distilled water (10% ethanol or water) to remove the unbound MUA and citrate. The assay consisted of adding 10 µL of the test sample to 200 µL of the nAu-MUA suspension, followed by the addition of 10 µL of 100 mM HCl (MilliporeSigma Canada Ltd., Oakville, Canada). To investigate the responsiveness of the assay to various

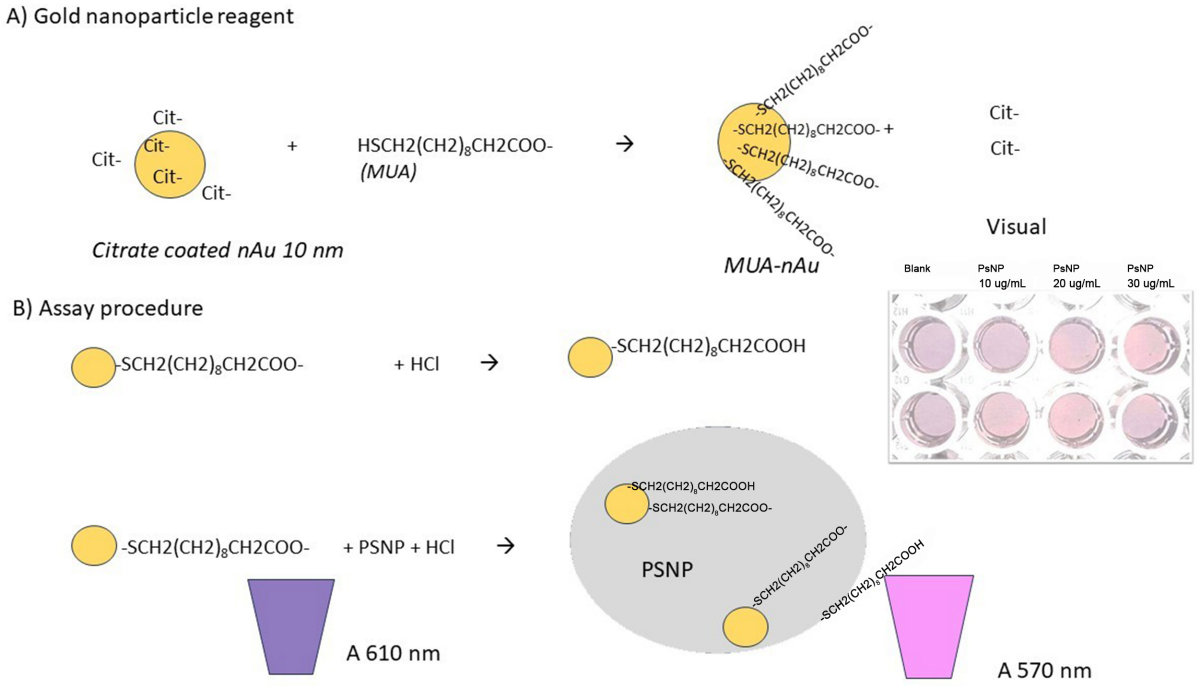

Figure 1. Methodology overview for the nAu sensor for the detection of NPs. Gold nanoparticles (nAu) of 10 nm diameter are first labeled for 24 hr to mercaptoundecanoic acid (MUA) to form nAu-MUA (A). The nAu-MUA complexes are separated from unreacted MUA by centrifugation and resuspension in 10% ethanol. The nAu-MUA is colored violet in the presence of 5 mM HCl in the absence of NPs (B). When it binds to the hydrophobic NPs, the violet color (610 nm) changes to a red wine color (550-580 nm) in a concentration-dependent manner[16]. MUA: Mercaptoundecanoic acid; NPs: nanoplastics; nAu: nanogold.

types of plastics, we examined the following types of plastics: PsNP of different sizes (20, 50, and 100 nm diameter), polyethylene terephthalate (PET) leachates from a 4-year-old water bottle, and tire wear nanoparticles (TWNP) leachates. The different sizes of PsNPs were examined to determine the influence of size on the plasmonic signals at 523 and 610 nm (see below). The TWNP leachates were prepared from drilling dust in new tires with a diamond-coated drilling probe (0.5 cm diameter) and from an ethanol-based commercial formulation of recycled used tire crumbs (particle size: 0.5-1 mm, 40 mg/mL) as previously described[20]. This suspension was exposed to the following cycle three times: frozen at -85 °C, thawed at RT, and sonicated for 1 h on the highest setting. Then, the suspension was filtered through a 0.22 µm cellulose membrane and kept at RT until analysis. For PET water bottles, the bottles (150 mL) were left on a shelf for 4 years under normal light (12-10 h) and dark diurnal (12-14 h) cycles. The bottles were then opened, filtered on a 0.22 µm pore filter and the sample was analyzed directly (no addition of ACN). Without NPs, the addition of HCl causes the bright red color of the nAu-MUA solution (523 nm) to shift to a dark purple color (610 nm). This purple color indicates aggregation of nAu-MUA complexes, whereas monomeric nAu-MUA appears light red. When NPs are present under aggregation conditions (HCl), the nAu-MUA complexes interact with the hydrophobic surface of the NPs, thereby limiting aggregation of the nAu-MUA complex. A blue shift in the absorbance from the aggregated form of the nAu-MUA complex at 610 nm to 560-590 nm indicates increased distance between aggregated nAu-MUA by interaction with NPs[21]. After 5 min, the absorbance (plasmon resonance) was measured (523, 570, and 610 nm) using both a microplate reader (model: Synergy-4, Bioteck Instruments, Winooski, USA) and a Samsung smartphone camera using a free application (RGB color detector) for color analysis (R band). This application analyzes the intensity in the R band of the sample from the picture taken. The limit of detection (blank standard deviation × 2) was estimated at 8 µg/mL for the 50 nm diameter PsNP, which corresponds to tissue

concentrations in the order of 50 ng/mg tissues.

Extraction and detection of NPs from mussel homogenates

As stated before, this method was further adapted for biological mussel tissues by conducting a preliminary salting-out extraction of NPs using saturated NaCl (5 M)/ACN[19]. The freshwater mussels were collected at a reference site, a pristine lake 100 km north in the Laurentians area, far from anthropogenic activity. Following an acclimation period of 3 weeks, they were caged (from July to October 2017) at the following sites: (1) a rainfall overflow site (OVF); (2) a site 15 km downstream from the center of Montréal, QC, Canada (Down-city); and (3) a site in the Saint-Lawrence River 8 km downstream of the municipal effluent dispersion plume of the city of Montréal (Down-Effluent). We also selected Down-Effluent, a site where wastewater treatment occurs and where a lower plastic exposure is expected. For each site, three cages containing 20 mussels were placed at 1 m depth. At the end of the 3-month exposure period, mussels were brought back to the laboratory (Montréal, Québec, Canada) and purged in clean water overnight at 15 °C, and their digestive glands were excised and homogenized in Hepes-NaOH buffer (10 mM, pH 7.4) containing 100 mM NaCl, 1 μg/mL aprotinin (protease inhibitors; MilliporeSigma Canada Ltd. Oakville, Canada) and 1 mM ethylenediaminetetraacetic acid (EDTA). The homogenates were centrifuged at 2,500 × *g* (5 min, 20 °C) to remove large tissue debris. The extraction procedure was carried out as follows: the supernatant was mixed with 2 volumes of saturated 5 M NaCl followed by 0.5 volume of ACN. After 15-30 min mixing, the sample was centrifuged (1,500 × *g*, 5 min) to separate the organic phase (upper phase) from the aqueous (lower phase). Preliminary experiments with fluorescently labeled PsNPs (50 to 100 nm) showed that NPs readily partitioned (> 98%) in ACN in high salt conditions. For the detection assay, 200 μL of the nAu-MUA suspension was mixed with 10 μL of samples, and the color changes were measured as described above. Preliminary experiments also revealed that ACN did not influence the reaction process (color changes) and could replace ethanol at 5% concentration [Table 1]. Blanks and additions of PsNPs in the homogenate fractions were prepared in the presence of ACN for method validation [Table 2].

Refractive index, neutral lipids, and amyloid estimations

The changes in RI and TRR were also determined in the digestive gland fractions (10,000 × *g*, 20 min, 2 °C). The levels of proteins were determined in the homogenate and in S10 digestive gland fractions (10,000 × *g*, 30 min, 4 °C) using the Coomassie blue dye binding principle, and bovine serum albumin was used for calibration[22]. The RI was directly measured in homogenate fractions (between 8 and 16 mg/mL protein concentration) as described above. To measure the TRR, the homogenate samples were diluted to 1 mg/mL in PBS and 1 mM of DTNB was added and 412 nm absorbance changes followed for 40 min as described above[18].

The levels of neutral lipids were determined in the homogenates using Nile red dye[23]. Briefly, a 20 μL of the homogenates was mixed with 200 μL of Nile red dye (10 μM, in PBS) and fluorescence was measured (excitation 485 nm, emission 520 nm) with a fluorometer (model: TB-380, Turner Biosystems, San Jose, USA). Calibration was achieved using 0.01% Tween-20 and the data were expressed as mg lipids/mg proteins.

The levels of amyloid proteins were estimated by the centrifugation methodology using Congo red (MilliporeSigma Canada Ltd. Oakville, Canada) as previously described[24]. The principle of the assay resides in the observation that amyloid proteins (insoluble in saline media such as PBS but soluble in distilled water) decrease the absorbance of the dye at 490 nm in a concentration-dependent manner. Briefly, the homogenate 1,500 × *g* fraction was centrifuged at 10,000 × *g* for 10 min and the pellet resuspended in PBS. This process was repeated 4 more times, and the pellet was washed once in distilled water and centrifuged

Table 1. Comparison of the nAu-MUA methodology in the presence of EtOH or ACN

Added PsNP	Absorbance[1] (λ = 570 nm)	Absorbance[2] (λ = 570 nm)	RI[2]
0.0 mg/mL (blank)	0.00	0.00	1.3365
0.6 mg/mL	0.10	0.09	1.3362
1.3 mg/mL	0.15	0.13	1.3363
2 mg/mL	0.23	0.21	1.3363

[1]Final concentration of EtOH = 10%; [2]Final concentration of ACN = 5%. ACN: Acetonitrile; PsNP: polystyrene nanoplastic; RI: refractive index.

Table 2. Calibration of the nAu-MUA assay for PsNPs

Concentration	R signal	Absorbance (λ = 570 nm)	RI	Extrapolated concentration	Concentration standard addition
Direct calibration (external)					
0 (blank)	162	0.00	1.3362		
20 µg/mL	168	0.04	1.3365		
40 µg/mL	174	0.07	1.3363		
60 µg/mL	193	0.10	1.3363		
Standard addition (internal)					
0 (sample)	170			30	27.4 µg/mL
+20 µg/mL	176			53	
+40 µg/mL	181			63	
+60 µg/mL	189			97	

Calibration of the nAu-MUA assay in the presence of 5% ACN using external and standard addition calibration. The detection limit of the assay was determined at 9 µg/mL based on 2 × standard deviations of the blank samples. ACN: Acetonitrile; MUA: mercaptoundecanoic acid; nAu: nanogold; PsNPs: polystyrene nanoplastics; RI: refractive index.

again. The pellet was resuspended once more in distilled water to release amyloids and centrifuged again. The presence of amyloids was determined by the decrease in absorbance at 490 nm (1/490 nm) after adding 10 µM Congo Red in the supernatant and the data were expressed as the inverse of the absorbance/mg proteins in the digestive gland.

The levels of aldehydes were determined in the 10,000 × *g* supernatant of the homogenate using the 4-amino fluorescein fluorescence methodology[25]. Briefly, 20 µL of S10 fraction was mixed with 200 µL of 10 µM 4-aminofluorescein (MilliporeSigma Canada Ltd., Oakville, Canada) in PBS and the fluorescence was taken at 485 nm excitation and 520 nm emission. The data were expressed as relative fluorescence units/mg total proteins. The instrument sensitivity was calibrated with an external standard of 1 µM fluorescein (to 1,000 fluorescence units; supplied with the instrument package).

Data analysis

The experiments were repeated 3 times (n = 3), and the data were presented as mean (± standard error). The data were subjected to the Kruskal-Wallis non-parametric analysis of variance followed by the multiple comparison Conover-Iman test to find differences between groups. Only differences with the reference site were discussed. Correlation analysis was performed using the Pearson-moment procedure. All statistical tests were performed using the StatSoft software package (version 13). The level of significance α of 0.05 was used.

RESULTS AND DISCUSSION

In this study, we adapted and used a simple visualization assay using a nAu sensor probe[16] to assess the exposure of mussels *in situ* to different urban effluents. In addition, we investigated the effects of NPs *in vitro* on the RI and the TRR in an albumin-rich solution and tested these markers, along with neutral lipids and amyloids, in mussels exposed to urban pollution.

Methodological improvement of the nAu-MUA assay

The levels of NPs were determined in biological tissues using the nAu-MUA assay initially developed for the estimation of plastics in simple matrices such as water or plastic tea bag leachates[16]. However, more complex matrices such as digestive gland homogenates inevitably require a primary fractionation step. Therefore, a simple salting-out extraction was designed in the presence of ACN to recuperate NPs in mussel tissues. The nAu-MUA assay was tested in the presence of ACN (5% final concentration). The absorbance at 570 nm and the R color measurements were taken directly in microplates with a smartphone camera or a microplate reader [Table 1]. The absorbance did not change compared to the original method (10% ethanol), suggesting that ACN could also be a suitable solvent for this assay. Additionally, the RI did not change with the addition of PsNPs to nAu-MUA reagent, suggesting negligible aggregation of nAu-MUA. The calibration data revealed that the R color (and the absorbance at 570 nm) increased with the addition of increasing concentrations of PsNPs [Table 2]. Calibration by the standard addition method of a spiked tissue sample revealed the same results as the external calibration method, with regression coefficients ranging from 0.96 to 0.99 [Table 2]. For the standard addition calibration, the test sample was a NaCl/ACN extract of the digestive gland of mussels *E. complanata*. The estimated concentration of PsNPs in the sample was estimated at 30 and 27 µg/mL with the direct and standard addition methodologies, respectively. This suggests that the extraction of PsNPs in ACN from tissues did not introduce important matrix effects. The aggregation of nAu-MUA could be favored by the presence of salts at concentrations over 10 mM, such as HCl or NaCl[16,26]. However, the assay was conducted in ACN fraction devoid of salts. The saturated NaCl/ACN extraction is based on the salting out of large molecules. In this context, less dense plastic particles (usually 0.75-0.95 g/mL) will tend to float at the surface. The ACN step will extract and concentrate these lighter particles. Larger molecules such as peptides/proteins and other large molecules (humic and fulvic acids present in natural organic matter in surface waters) would then precipitate during the centrifugation step[27]. Although the ACN can extract less polar organic compounds (e.g., neutral lipids) along with PsNps (20 to 100 nm in diameter), interference from large amounts of neutral lipids could interfere in the distances between the nAu-MUA-NPs complex. However, significant differences between the direct calibration method and the standard addition method were not found, suggesting the absence of interferences in the conditions used in this study. Moreover, changes in lipids in digestive gland homogenates were not significantly correlated with NPs as determined by the plasmonic nAu-MUA assay. Interference from dissolved organic matter (> 15 mg/L) was observed with the nAu-MUA assay when used directly on surface water samples[27]. In amounts exceeding 15 mg/L, only 15%-20% of the NPs were detected when the assay was used directly on the water samples. An extraction step should be considered when the assay is to be applied directly to the sample with high levels of dissolved organic carbon, as used in the present study.

Responsiveness of the nAu-MUA assay to various plastics

The nAu-MUA assay was tested against various types of plastics such as PsNPs (20, 50, and 100 nm), water from 4-year-old PET water bottles, and tire/recycled tire leachates [Table 3]. As expected, the test responded to PsNPs. Tire wear leachates also elicited a contrasted positive signal compared to the blanks, suggesting that this assay also responds to petroleum-based rubber materials from tire wear and recycled tires. The nAu-MUA assay was tested on water from 4-year-old PET drinking water bottles and the assay also detected the presence of NPs. The nAu-MUA assay responded well to different types and sizes of plastics such as PS, rubber (tire), and PET. The detection of NPs in water bottles corroborates previous findings[16],

Table 3. Response of the nAu-MUA assay to various types of plastics

Materials[1]		Response factor[2]
Blank		1.00
Distilled water		1.00
PsNPs	20 nm[3]	1.21
	50 nm[3]	1.17
	100 nm[3]	1.20
Tire wear particle leachates[4]		1.20
Tire crumb[4]		1.14
Water from 4-years-old PET bottle[5]		1.17

[1]10 µL of sample added to 200 µL nAu-MUA; [2]Obtained by dividing the R color sample by the R color blank; [3]15 µg/mL standard solutions; [4]400 µg of ethanol tire wear and aged recycled tire rubber (crumb) powders (1 g/10 mL ethanol); [5]See material and method for details. Note: no extraction or concentration step. MUA: Mercaptoundecanoic acid; nAu: nanogold; PET: polyethylene terephthalate; PsNPs: polystyrene nanoplastics.

i.e., NPs < 100 nm are released from plastic bottles. This assay also proved to work with polypropylene and polyethylene (tea bags) samples and seemed unaffected by the positive or negative charges at the surface of PsNPs, which are likely to be found in aged plastics.

Detection of NPs in mussel digestive glands

The relative levels of NPs were determined in the extract of the digestive gland of the freshwater mussel *E. complanata* following 3 months of caging experiments at various sites in the province of Québec (Canada). We observed a significantly ($P < 0.05$) higher signal for the nAu-MUA assay at the three sites compared to the control [Table 4]. The data revealed that mussels caged 15 km downstream from the city center of Montréal had higher levels of NPs compared to the reference site, in which a very low signal was detected. The levels of NPs were lower in the municipal effluent dispersion plume and were similar to the ones at the overflow site. These results indicate that plastic contamination arises in every site, but more importantly, downstream urban areas, and to a lesser extent, rainfall overflow sites draining nearby roads (tire wear and asphalt erosion) and municipal effluents. In a previous study with caged mussels, similar observations were found in mussels exposed to combined sewer overflows and municipal effluents using size exclusion gel chromatography and fluorescence detection using a molecular rotor probe for NPs in tissues[28]. Increased detection of microplastics and NPs was found in irrigated edible plants downstream municipal wastewater[29]. Interestingly, although plastics are found in most lakes and river samples, their levels were increased at sites close to urban pollution, including street runoffs in combined sewer overflows. The lower NP signals in the digestive gland extracts of mussels exposed to municipal effluent compared to Down city suggest that wastewater treatment retains NPs during the process. Following wastewater treatments, levels of MPs and NPs were shown to be drastically reduced compared to the raw influent wastewater in two different municipal effluents[30]. In this study, the removal of MPs (from 26 to 1.75 µg/L) and NPs (from 12 to 0.71 µg/L) represented diminutions of 93% and 94%, respectively. Although proportions of NPs (particle size: 0.01 to 1 µm) were similar in both effluents, the removal efficiency was least effective with NPs (< 1 µm) compared to MPs (> 1 µm). In another study on larger MPs, the average abundance of MP in the influent was lowered (from 196 to 9 particles/L), which represents efficiency between 90% and 97%[31]. These observations indicate that the removal of MPs by the wastewater treatment plant, yet incomplete, cannot be ignored. This is consistent with the low levels of NPs in the digestive glands of mussels caged downstream of the municipal effluent plume observed in our study compared to the highest downstream of the city site. Another explanation could be that a lowered filtration rate leading to reduced uptake by mussels could also explain the discrepancy observed between both sites. However, this was not evaluated in our study. Decreased filtration rates and acetylcholinesterase activity were found in

Table 4. Case study with caged lake mussels downstream a large city, rainfall overflow, and municipal treated effluent in the Saint-Lawrence River

Caging sites	nAu-MUC method (µg/g)	Lipid (mg/g tissue)	Aldehydes (RFU/mg proteins)	Amyloids 1/ (Abs × mg proteins)
Reference lake	0.02 ± 0.01	16 ± 3 h	110 ± 30	4.9 ± 0.02 h
Down-city	0.11 ± 0.01*	31 ± 5*	200 ± 30*	4.7 ± 0.47 h
Down-Effluent	0.05 ± 0.02*	21 ± 5 h	450 ± 53*	4.3 ± 0.20 h
OVF	0.06 ± 0.01*	21 ± 3*	330 ± 27*	5.5 ± 0.04*

Comparisons were made with the control site. *$P < 0.05$. nAu: Nanogold; OVF: overflow site.

clams exposed to 80 nm NPs, 6 µm MPs, and ciprofloxacin[32]. Ciprofloxacin, an antibiotic found in municipal wastewater, was shown to worsen the inhibition potential of NPs when co-administered to clams. In another study, marine mussels exposed to elevated PsNP concentrations (0.5 and 5 mg/L) had total antioxidant capacity and acetylcholinesterase activity induced and inhibited, respectively[33]. Acetylcholinesterase activity is usually coupled with filtration rates, indicating that reduced filtration rates could represent an adaptive mechanism to limit exposure and damage caused by NPs. Although not as contrasted as the Down-city site, the overflow site also showed significantly higher NP detection in the mussel digestive glands. This observation suggests that the combined excess of rain and untreated wastewater also contributes to the NPs burden of mussels. The release of NPs from asphalt and tire erosion could also be a contributor to the levels of NPs observed in our study.

Biological and biochemical markers in the mussel digestive glands

In addition to NPs, other biomarkers such as the RI, TRR, aldehydes, neutral lipids, and amyloids in the digestive gland fractions were assessed. Globally, exposure of mussels to urban pollution increased levels of lipids, aldehydes, RI (digestive gland homogenates), and denatured proteins (amyloids). Their levels were highest at the rainfall overflow and downstream the city center sites for lipids and amyloid levels [Table 4]. In our study, we observed a significant increase in neutral lipids at the overflow site and downstream of the city, but not following exposure to the wastewater effluent site [Table 4]. Furthermore, an increased signal for aldehyde formation was observed at all sites [Table 4]. We observed that the RI was significantly lower in mussels downstream of the city as shown below. Interestingly, the highest levels of NPs were also found at this same site. In our study, we also noticed a significant increase in the amyloid contents in mussels exposed to the overflow site [Table 4]. Amyloid formation is involved in several degenerative diseases as a result of a long-term accumulation of oxidatively denatured protein plaques in various tissues and organs[15] (e.g., brain, muscle, and liver) and was referred to as a typical cellular disorder in the physiopathology of aging[34]. To this date, we ignore why amyloids were increased in these mussels, but we observed a significant correlation between amyloids and the RI ($r = 0.66$; $P < 0.01$). This observation strengthens the possible association between these two markers in the digestive gland homogenates.

In vitro investigations of effects of PsNPs in albumin-rich solution and biological matrices

To further investigate the observed changes in the RI and TRRs following exposure to NPs, we conducted an exploratory *in vitro* test to determine the effects of PsNPs on RI and TRRs in an albumin-rich solution and the digestive gland homogenates of *E. complanata* [Figure 2A-D]. Thus, a concentrated albumin solution was prepared at 100 mg/mL near the reported density of intracellular environments[18] and spiked with increasing concentrations of PsNPs. The presence of 50 nm PsNPs decreased the RI of the albumin solution in a concentration-dependent manner (between 0 and 0.15 µg/L, Figure 2A). It is important to state that the addition of PsNPs (without albumin) did not influence the RI of the solution. Furthermore, the TRRs in albumin-rich solutions were determined and revealed a decrease in the reaction rates when over

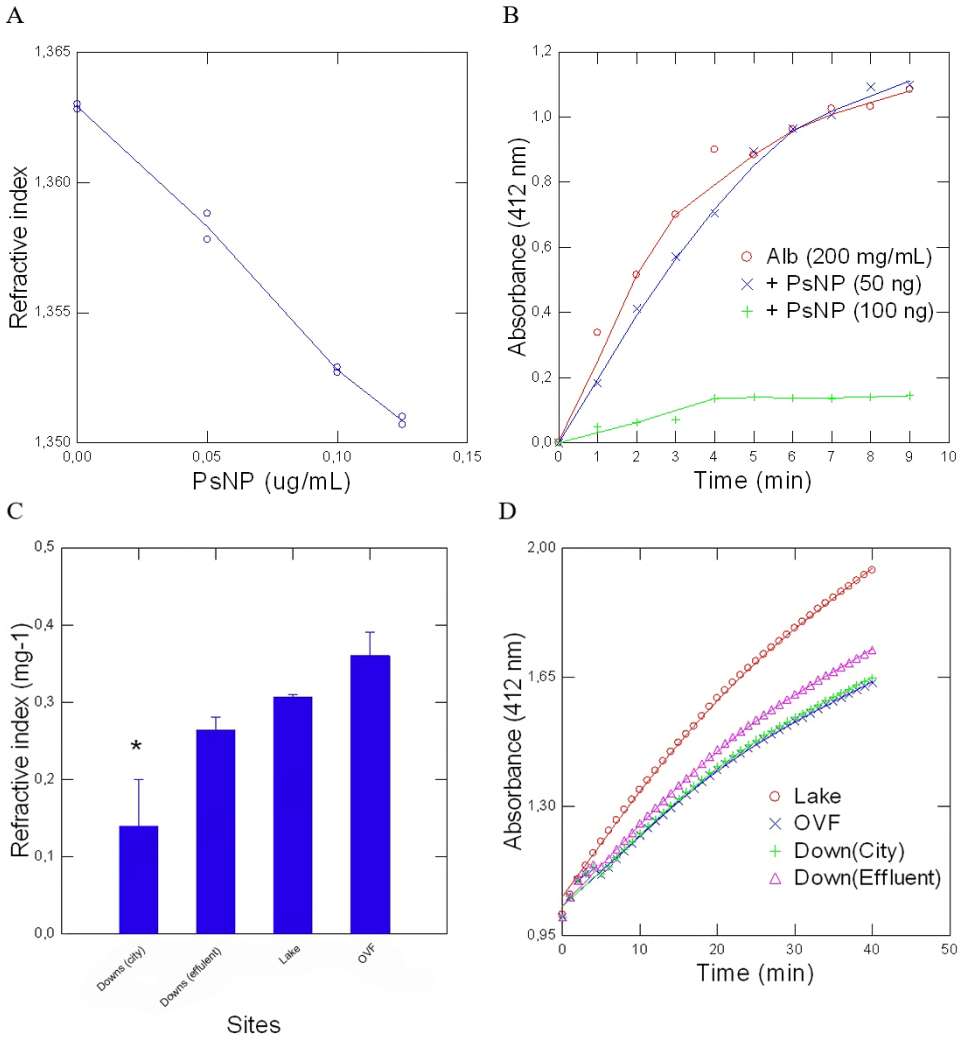

Figure 2. Refractive indexes and TRR following *in vitro* exposure to plastic nanoparticles (A and B) or in *E. complanata* digestive gland extracts following *in situ* exposures (C and D). The RI (A) and the TRR (B) were determined in concentrated albumin solutions. Mussels were encaged for 3 months at various sites and dissected, and digestive glands homogenates were assessed for RI and TRR. OVF: Overflow site; PsNP: polystyrene nanoplastic; RI: refractive index; TRR: thiol-reaction rates.

100 ng of PsNPs were added [Figure 2B]. In turn, this rearrangement could lower the free albumin in the dissolved phase and explain the decreased RI. Overall, these results obtained in albumin-rich solutions contribute to a better understanding of the effects of NPs in protein-rich samples and strengthen the link between the effects of NPs and the biological and biochemical effects observed in the exposed mussel's digestive gland homogenates.

Indeed, albumin could interact with PsNPs, forming local and dense albumin-coated PsNP clusters that restrict the diffusion of substrates[9,35]. Analysis of the reaction rates revealed that the reaction rates over time (a measure of the spectral dimension of the reaction in crowded environments[9]) decreased more strongly in mussels downstream of the urban area compared to the reference lake (results not shown), consistent with the formation of elongated aggregate arrangements of percolation organization. Similarly, TRR could be decreased by the rearrangement of albumin in the presence of PsNPs and perhaps by a non-specific binding of the reagent on the hydrophobic surface of PsNPs. Additionally, the RI and the TRR were also

measured in the digestive gland extracts [Figure 2C and D]. The analysis revealed that the RI of the homogenate (normalized to protein content) was significantly decreased at the site with the highest levels of NPs (downstream city center site). Although other contaminants might be at play in these complex environments, it is plausible that NPs contribute to the decreased RI as a result of alteration in protein organization and reaction rates in the digestive gland extracts. Such changes in protein organization were also measured by anisotropic changes in the digestive gland homogenates, consistent with nematic crystal formation in mussels exposed to PsNPs and municipal effluents[36]. The complexation of albumin to PsNPs was previously shown to result from the hydrophobic environment of both albumin and PsNPs[37] and could be positively influenced by the presence of anionic charges on the surface of PsNPs[38]. This complexation is likely to happen given the local cationic patch that albumin displays on its surface and the hydrophobic environment of the NPs, especially when anionic charges are present on aged/weathered NP surfaces. Anionic charges ($R\text{-}COO^-$) were reported to form during the weathering/degradation of plastic materials by UV and ozone[10]. The addition of these anionic charges on the surface of NPs could expectedly weaken the interaction with anionic natural organic matter (e.g., humic acids and alginates) and support interactions with cationic proteinaceous compounds usually found in wastewater. Ultimately, these interactions with NPs could lead to spatial changes in proteins and protein networks and consequently alter enzyme activity. Such influence of PsNPs on the enzymatic activity of LDH was previously reported *in vitro* and mussels exposed to PsNPs[13]. The changes in LDH activity by these NPs were consistent with the altered fractal organization of complex protein networks. Indeed, the calculated fractal dimension of LDH reaction rate was reduced by PsNPs as with F-actin, the natural ligand for LDH, suggesting a loss of affinity for its substrate pyruvate and NADH (increased affinity constant K_M). Indeed, the spectral dimension of the reaction rates reached 1.2, also indicative of a percolation structure (continuous linear dust fragments). Thus, NPs interacting with albumin or protein networks in cells would form percolation-like structures, leading to reduced RI and TRR.

CONCLUSION

In this study, we adapted a simple extraction and detection method for NPs, and we investigated the *in situ* exposure of the freshwater mussel *E. complanata* in polluted urban environments. We also assessed the biochemical effects using several simple markers in exposed mussels and conducted an exploratory *in vitro* test to further understand the effects of NPs in protein-rich samples. Our results suggest that mussels exposed to city effluents are exposed to NPs and show disorders typical of NP exposure. Overall, *E. complanata* proved to be a potential surrogate for NP contamination in biomonitoring studies and responded to various effluents. Given that plastic pollution is ubiquitous and that the traditional NP detection methods (e.g., pyrolysis gas chromatography, thermogravimetric Fourier transformation spectrometry, transmission electron microscopy[39]) are labor- and cost-extensive, the access to quick and cheap assessment methods for the monitoring of plastic contamination and effects are needed. Although this method will need further validation, this study contributes to the development of new accessible tools for institutions and opens new perspectives for preliminary screening strategies to tease out sites with high levels of NPs.

DECLARATIONS

Acknowledgments

The authors are thankful to the Saint-Lawrence Action Plan and Plastics research initiative of Environment and Climate Change Canada for supporting this research. The technical assistance for the mussel caging experiments of Hiba Qchiqach is duly recognized in this project.

Authors' contributions

Conceptualization, methodology, validation, formal analysis, investigation, writing - original draft: Gagné F
Experimentation, analysis, writing -review and editing: Gagné F, Gauthier M, André C
Conceptualization, supervision, resources: Gagné F

Availability of data and materials

Not applicable.

Financial support and sponsorship

None.

Conflicts of interest

All authors declared that there are no conflicts of interest.

Ethical approval and consent to participate

Not applicable.

Consent for publication

Not applicable.

REFERENCES

1. Jiang B, Kauffman AE, Li L, et al. Health impacts of environmental contamination of micro- and nanoplastics: a review. *Environ Health Prev Med* 2020;25:29. DOI
2. Eriksen M, Lebreton LCM, Carson HS, et al. Plastic pollution in the world's oceans: more than 5 trillion plastic pieces weighing over 250,000 tons afloat at sea. *PLoS One* 2014;9:e111913. DOI
3. Koelmans AA, Mohamed Nor NH, Hermsen E, Kooi M, Mintenig SM, De France J. Microplastics in freshwaters and drinking water: critical review and assessment of data quality. *Water Res* 2019;155:410-22. DOI
4. Fang C, Luo Y, Naidu R. Microplastics and nanoplastics analysis: options, imaging, advancements and challenges. *TrAC Trend Anal Chem* 2023;166:117158. DOI
5. Lee J, Chae KJ. A systematic protocol of microplastics analysis from their identification to quantification in water environment: a comprehensive review. *J Hazard Mater* 2021;403:124049. DOI
6. Chen Z, Liu X, Wei W, Chen H, Ni BJ. Removal of microplastics and nanoplastics from urban waters: separation and degradation. *Water Res* 2022;221:118820. DOI
7. Kik K, Bukowska B, Sicińska P. Polystyrene nanoparticles: sources, occurrence in the environment, distribution in tissues, accumulation and toxicity to various organisms. *Environ Pollut* 2020;262:114297. DOI
8. Aon MA, Cortassa S, Lloyd D. Chaotic dynamics and fractal space in biochemistry: simplicity underlies complexity. *Cell Biol Int* 2000;24:581-7. DOI
9. Gagné F. Ecotoxicology of altered fractal organization in cells. *Am J Biomed Sci Res* 2020;8:498-502. DOI
10. Li X, Ji S, He E, et al. UV/ozone induced physicochemical transformations of polystyrene nanoparticles and their aggregation tendency and kinetics with natural organic matter in aqueous systems. *J Hazard Mater* 2022;433:128790. DOI
11. Khago D, Bierma JC, Roskamp KW, Kozlyuk N, Martin RW. Protein refractive index increment is determined by conformation as well as composition. *J Phys Condens Matter* 2018;30:435101. DOI
12. Wen J, Arakawa T. Refractive index of proteins in aqueous sodium chloride. *Anal Biochem* 2000;280:327-9. DOI
13. Auclair J, Gagné F. The influence of polystyrene nanoparticles on the fractal kinetics of lactate dehydrogenase. *Biochem Biophys Rep* 2020;23:100793. DOI
14. Capolupo M, Gunaalan K, Booth AM, Sørensen L, Valbonesi P, Fabbri E. The sub-lethal impact of plastic and tire rubber leachates on the Mediterranean mussel *Mytilus galloprovincialis*. *Environ Pollut* 2021;283:117081. DOI
15. Cabaleiro-Lago C, Szczepankiewicz O, Linse S. The effect of nanoparticles on amyloid aggregation depends on the protein stability and intrinsic aggregation rate. *Langmuir* 2012;28:1852-7. DOI
16. Zhou H, Cai W, Li J, Wu D. Visual monitoring of polystyrene nanoplastics < 100 nm in drinking water based on functionalized gold nanoparticles. *Sens Actuators B Chem* 2023;392:134099. DOI

17. Savageau MA. Development of fractal kinetic theory for enzyme-catalysed reactions and implications for the design of biochemical pathways. *Biosystems* 1998;47:9-36. DOI
18. Butterworth PHW, Baum H, Porter JW. A modification of the Ellman procedure for the estimation of protein sulfhydryl groups. *Arch Biochem Biophys* 1967;118:716-23. DOI
19. Gagné F. Isolation and quantification of polystyrene nanoplastics in tissues by low pressure size exclusion chromatography. *J Xenobiot* 2022;12:109-21. DOI
20. Xu EG, Lin N, Cheong RS, et al. Artificial turf infill associated with systematic toxicity in an amniote vertebrate. *Proc Natl Acad Sci U S A* 2019;116:25156-61. DOI
21. Reinhard BM, Siu M, Agarwal H, Alivisatos AP, Liphardt J. Calibration of dynamic molecular rulers based on plasmon coupling between gold nanoparticles. *Nano Lett* 2005;5:2246-52. DOI
22. Bradford MM. A rapid and sensitive method for the quantitation of microgram quantities of protein utilizing the principle of protein-dye binding. *Anal Biochem* 1976;72:248-54. DOI
23. Greenspan P, Mayer EP, Fowler SD. Nile red: a selective fluorescent stain for intracellular lipid droplets. *J Cell Biol* 1985;100:965-73. DOI
24. Pras M, Schubert M, Zucker-Franklin D, Rimon A, Franklin EC. The characterization of soluble amyloid prepared in water. *J Clin Invest* 1968;47:924-33. DOI
25. Xing Y, Wang S, Mao X, Zhao X, Wei D. An easy and efficient fluorescent method for detecting aldehydes and its application in biotransformation. *J Fluoresc* 2011;21:587-94. DOI
26. Choi I, Lee LP. Rapid detection of Aβ aggregation and inhibition by dual functions of gold nanoplasmic particles: catalytic activator and optical reporter. *ACS Nano* 2013;7:6268-77. DOI
27. Pirade F, Lompe KM, Jiménez-lamana J, et al. How suitable is the gold-labelling method for the quantification of nanoplastics in natural water? *AQUA Water Infra Ecosyst Soc* 2023:jws2023278. DOI
28. Gagné F, Roubeau-Dumont E, André C, Auclair J. Micro and nanoplastic contamination and its effects on freshwater mussels caged in an urban area. *J Xenobiot* 2023;13:761-74. DOI
29. Naziri A, Mina T, Manoli K, et al. Looking into the effects of co-contamination by micro(nano)plastics in the presence of other pollutants on irrigated edible plants. *Sci Total Environ* 2023;892:164618. DOI
30. Xu Y, Ou Q, Wang X, et al. Assessing the mass concentration of microplastics and nanoplastics in wastewater treatment plants by pyrolysis gas chromatography-mass spectrometry. *Environ Sci Technol* 2023;57:3114-23. DOI
31. Xu X, Jian Y, Xue Y, Hou Q, Wang LP. Microplastics in the wastewater treatment plants (WWTPs): occurrence and removal. *Chemosphere* 2019;235:1089-96. DOI
32. Guo X, Cai Y, Ma C, Han L, Yang Z. Combined toxicity of micro/nano scale polystyrene plastics and ciprofloxacin to *Corbicula fluminea* in freshwater sediments. *Sci Total Environ* 2021;789:147887. DOI
33. Wang X, Shao S, Zhang T, Zhang Q, Yang D, Zhao J. Effects of exposure to nanoplastics on the gill of mussels *Mytilus galloprovincialis*: an integrated perspective from multiple biomarkers. *Mar Environ Res* 2023;191:106174. DOI
34. Nezelof C. Role of defective intracellular proteolysis in human degenerative diseases. *Bull Acad Natl Med* 2102;196:1587-98. DOI
35. Fang Y, Li H, Ai N, Luo W. Fractal diffusion in a chemical space. *Int J Nonlinear Sci Numer Simul* 2000;1:235-8. DOI
36. Gagné F, Auclair J, André C. Polystyrene nanoparticles induce anisotropic effects in subcellular fraction of the digestive system of freshwater mussels. *Cur Top Toxicol* 2019;15:43-8. Available from: http://www.researchtrends.net/tia/article_pdf.asp?in=0&vn=15&tid=50&aid=6351. [Last accessed on 20 Dec 2023].
37. Kowalczyńska HM, Nowak-Wyrzykowska M, Szczepankiewicz AA, et al. Albumin adsorption on unmodified and sulfonated polystyrene surfaces, in relation to cell-substratum adhesion. *Colloids Surf B Biointerfaces* 2011;84:536-44. DOI
38. Simončič M, Hritz J, Lukšič M. Biomolecular complexation on the “wrong side”: a case study of the influence of salts and sugars on the interactions between bovine serum albumin and sodium polystyrene sulfonate. *Biomacromolecules* 2022;23:4412-26. DOI
39. Jung S, Raghavendra AJ, Patri AK. Comprehensive analysis of common polymers using hyphenated TGA-FTIR-GC/MS and Raman spectroscopy towards a database for micro- and nanoplastics identification, characterization, and quantitation. *NanoImpact* 2023;30:100467. DOI